Journal of Biomedical Materials Research Part A

Autologous bone marrow stromal cells loaded onto porous gelatin scaffolds containing Drynaria fortunei extract for bone repair

Journal:	*Journal of Biomedical Materials Research: Part A*
Manuscript ID:	JBMR-A-11-0696.R2
Wiley - Manuscript type:	Original Article
Date Submitted by the Author:	n/a
Complete List of Authors:	Chen, Kuo-Yu; National Yunlin University of Science and Technology, Department of Chemical and Materials Engineering, Dong, Guo-Chung; National Health Research Institutes, Division of Medical Engineering Research Hsu, Chin-Yin; China Medical University, School of Chinese Medicine Chen, Yueh-Sheng; China Medical University, Institute of Chinese Medical Science Yao, Chun-Hsu; China Medical University, Department of Biomedical Imaging and Radiological Science
Keywords:	bone marrow stromal cells, Drynaria fortunei, gelatin, genipin, tricalcium phosphate

Autologous bone marrow stromal cells loaded onto porous gelatin scaffolds containing *Drynaria fortunei* extract for bone repair

No benefit of any kind will be received either directly or indirectly by the authors

Kuo-Yu Chen,[1] Guo-Chung Dong,[2] Chin-Yin Hsu,[3] Yueh-Sheng Chen,[3,4] Chun-Hsu Yao[3,4,*]

[1]Department of Chemical and Materials Engineering, National Yunlin University of Science and Technology, Yunlin, Taiwan

[2]Division of Medical Engineering Research, National Health Research Institutes, Miaoli, Taiwan

[3]School of Chinese Medicine, China Medical University, Taichung, Taiwan

[4]Department of Biomedical Imaging and Radiological Science, China Medical University, Taichung, Taiwan

*** Correspondence and reprint request to:**

Chun-Hsu Yao, School of Chinese Medicine, China Medical University, 91, Hsueh-Shih Road, Taichung 404, Taiwan; e-mail: chyao@mail.cmu.edu.tw

Tel: +886-4-22053366 ext. 7806; Fax: +886-4-2207-6976

Abstract: GGT-GSB composite was prepared by mixing a biodegradable GGT composite containing genipin-cross-linked gelatin and β-tricalcium phosphate with Gu-Sui-Bu extract (GSB) (*Drynaria fortunei* (Kunze) J. Sm.), a traditional Chinese medicine. Then, porous GGT and GGT-GSB scaffolds were fabricated using a salt-leaching method. The GGT and GGT-GSB scaffolds thus obtained had a macroporous structure and high porosity. Rabbit bone marrow stromal cells (BMSCs) were seeded onto GGT and GGT-GSB scaffolds. The biological response of rabbit calvarial bone to these scaffolds was considered to evaluate the potential of the scaffolds for use in bone tissue engineering. After 8 weeks of implantation, each scaffold induced new bone formation at a cranial bone defect, as was verified by X-ray microradiography. The BMSC-seeded GGT-GSB scaffolds induced more new bone formation than the BMSC-seeded GGT and acellular scaffolds. These observations suggest that an autologous BMSCs-seeded porous GGT-GSB scaffold can be adopted in bone engineering *in vivo* and has great potential for regenerating defective bone tissue.

Key Words: bone marrow stromal cells, *Drynaria fortunei*, gelatin, genipin, tricalcium phosphate

INTRODUCTION

Bone tissue engineering is an attractive approach for treating bone loss in various shapes and amounts. Successful repair of injured tissue using tissue engineering strategies depends on a 3D biodegradable scaffold, appropriate cells, and suitable culture conditions. Ideally, the scaffold should promote the migration of cells toward and into the scaffold during *in vitro* cell culture. After it is implanted into a bone defect, the scaffold must be reabsorbed naturally as the bone grows, until finally, it is completely replaced with newly formed bone.

Bone marrow stromal cells (BMSCs) have potential for use in bone tissue engineering owing to their general availability, great ability to self-renew, and favorable osteogenic potential.[1] In various animal models, the combination of autologous BMSCs and scaffolds has been demonstrated to promote bone repair.[2-5] Additionally, immunological responses are not a concern. The chemical composition of scaffold appears to be an important factor in regulating the adhesion, proliferation, and osteogenic differentiation of BMSCs. In recent years, many researchers have studied the combination of BMSCs with gelatin-based scaffolds for bone tissue engineering.[6-9] Moreover, a gelatin-based scaffold can serve as a vehicle for delivering osteoinductive agents to promote the healing of bone defects.[10]

In the authors' recent investigation, a biodegradable composite comprising genipin, a natural cross-linking reagent extracted from the fruit of *Gardenia jasminoides Ellis*, cross-linked gelatin/β-tricalcium phosphate (β-TCP) mixture was prepared as a bone substitute. The gelatin molecules and calcium ions, continuously released from the composite, promoted the differentiation and proliferation of the osteoblasts.[11] The results of *in vivo* evaluation demonstrate that the composite has high biocompatibility. However, the cross-linked composite has a lower porosity.[12]

Numerous traditional Chinese herbal medicines are frequently utilized to treat musculoskeletal disorders and have been shown to be effective for bone regeneration. Among

these, the dried rhizome of perennial pteridophyte *Drynaria fortunei* (Kunze) J. Sm., known as Gu-Sui-Bu (GSB), has been extensively used to treat bone-related diseases, such as bone fracture, osteoporosis, and arthritis, and has been demonstrated to have therapeutic effects in bone healing.[13] Research on GSB extract has established that it has a positive effect on the proliferation and differentiation of osteoblasts as well as bone cell activities *in vitro,* while it inhibits osteoclast formation.[14-21] In an earlier investigation, we found that adding GSB to composites of gelatin, genipin, and β-TCP accelerated bone regeneration.[14]

No research has been conducted on *in vivo* bone formation using a gelatin-based scaffold with a combination of BMSCs and GSB extract. In this study, a macroporous scaffold containing genipin-cross-linked gelatin and β-TCP (GGT) was prepared using a salt-leaching approach to carry GSB (GGT-GSB). BMSCs were harvested from healthy rabbits, expanded, and seeded onto the porous GGT and GGT-GSB scaffolds. The cell-seeded scaffolds were cultured in osteogenic induction medium and then incubated in a spinner flask. They were then autotransplanted into critically sized calvarial defects in rabbits to compare the bone repair potential of autologous BMSCs-loaded scaffolds with that of cells-free scaffolds, and to investigate the effects of GSB on bone formation *in vivo*. The radiographical and histological features of the transplants were evaluated.

MATERIALS AND METHODS

Preparation of GSB solution and porous GGT and GGT-GSB scaffolds

GSB was obtained from a local Chinese medicine store (Xing Long Pharmaceutical Co., Taichung, Taiwan) in dry form. Its identity was confirmed by experts in pharmacognosis. Aqueous GSB extract was prepared following a previously described method.[14] Briefly, a 100 g ground specimen of GSB was added to 500 mL of deionized water and boiled under reflux for 2 h. The aqueous extracts were filtered to remove insoluble debris and concentrated at

40°C by vacuum evaporation, before being freeze-dried to obtain the final powder. A 20 mg mL^{-1} GSB solution was obtained by dissolving the powder in deionized water.

The GGT scaffolds were prepared as described elsewhere.[22] Briefly, a homogeneous 18 wt % gelatin solution was obtained by dissolving porcine gelatin powder (Bloom number 300, Sigma, St. Louis, MO) in deionized water at 75°C. As the gelatin solution cooled to 50°C, genipin solution (Challenge Bioproducts, Yunlin, Taiwan) at a concentration of 0.5 wt % was added to form a cross-linking reaction at a constant temperature. After the solution was stirred for 2 min, β-TCP particles (Merck, Darmstadt, Germany) with grain sizes of 200–300 μm and sieved sodium chloride particles of size 250-470 μm were mixed with the gelatin-genipin mixture. The salt particles were dried in an oven at 170°C for 4 h before use. The weight ratio of gelatin to β-TCP and that of salt to gelatin/β-TCP/genipin composite were 1:3 and 3:1, respectively. Vigorous stirring made the mixtures increasingly viscous. They were poured into plastic dishes, allowed to solidify, and then frozen at –80°C for 30 min. The solidified composites were cut and shaped into cylindrical specimens of a particular size. The salt was caused to leach out completely by immersing the composites in deionized water for 24 h. During this period, the water was changed three times. Finally, the samples were frozen at –80°C for 24 h and lyophilized in a freeze dryer for another 24 h to form porous GGT scaffolds. The dried cylindrical scaffolds had a diameter of 15 mm and a thickness of 2 mm. The GGT-GSB scaffolds were prepared using an approach that was similar to that for preparing the GGT scaffolds. A homogeneous 18 wt % gelatin solution was obtained by dissolving gelatin powder in 20 mg mL^{-1} GSB solution instead of deionized water. The weight ratio of GSB to gelatin to β-TCP in the GGT-GSB scaffold was approximately 1:9:27. All samples were sterilized under gamma irradiation at 15 kGy before they were used.

Morphology of scaffolds

The cross-sectional morphology of scaffolds was examined under a Hitachi S-3000N (Japan)

scanning electron microscope (SEM). The test sample was frozen and dried following the aforementioned procedure. The dried sample was immediately sputter-coated with gold for further SEM observation. The average pore size in the cross-section was evaluated from measurements made from the pores in the SEM micrographs.

Evaluation of porosity

The porosity of the scaffold was determined using the Archimedes principle. The exterior volume (V_s) of each sample was measured using vernier calipers. The sample was then cut into pieces and immersed in a pycnometer containing deionized water. The actual volume (V_m) of the sample was calculated as $V_m = (W_w - W_0) - (W_t - W_p)$

where W_w is the weight of water and the pycnometer; W_0 is the weight of the dry pycnometer; W_t is the weight of water, the pycnometer and the sample fragments, and W_p is the weight of the dry pycnometer and dry sample fragments. The porosity was determined using the formula, Porosity (%) = $(V_s - V_m)/V_s \times 100$ (%). The values are given as mean ± standard deviation ($n = 6$).

Determination of *in vitro* degradation rate

To measure the rate of hydrolytic degradation of the scaffold, it was frozen, dried, and weighed (W_0). After the samples were soaked in 20 mL of deionized water for 1, 2, 4, 6, and 8 weeks at 37°C, they were retrieved from the deionized water, frozen, dried, and weighed (W_t). The percentage weight loss (ΔW (%)) was determined using the formula, ΔW (%) = $(W_0 - W_t)/W_0 \times 100$ (%). Determinations were made for four samples at each time point.

Isolation of BMSCs and cell culture

BMSCs were aspirated from the iliac crests of mature male New Zealand white rabbits that weighed 2.5–3.0 kg (and were purchased from the National Laboratory Animal Center, Taiwan) under total anesthesia. Before the beginning of the study, the ethical committee for

animal experiments at the Central Taiwan University of Science and Technology, Taichung, Taiwan, approved the protocols. Rabbits were anaesthetized intramuscularly with ketamine (Nang Kuang Pharmaceutical Co., Tainan, Taiwan) and 2% Rompun solution (Bayer, Germany) (1:1 ratio, 1.2 mL kg^{-1}) in an aseptic animal operation room. The aspiration syringe was wetted with sodium heparin (5000 U mL^{-1}, Chunghwa Chemical & Pharmaceutical Co., Taipei, Taiwan) to prevent clotting. Approximately 5 mL of bone marrow aspirates were harvested and added to low-glucose Dulbecco's modified Eagle's medium (L-DMEM; Gibco, Grand Island, NY) that was supplemented with 10% fetal bovine serum (FBS; Gibco), 1% penicillin/streptomycin (Gibco) and 3.7 g L^{-1} sodium bicarbonate. The cells were plated in a 75 cm^2 cell culture flask (Costar, Cambridge, MA) and incubated at 37°C under 5% CO_2. Each medium was changed after 24 h to remove non-adherent cells, and the adherent cells were reincubated. When cells cultured in flasks became almost confluent, the cells were detached using 0.25% trypsin/EDTA (Sigma) for 5 min at 37°C. Following primary culture, the cells were sub-cultured at 37°C under 5% CO_2. The culture medium was refreshed every 2 days. The cells at their second or third passage were used in the following experiments.

Rabbit BMSCs dynamically cultured with scaffolds

A dynamic culture system was employed to improve the exchange of nutrients and waste products between the interior and the exterior of the scaffold. In addition, it can provide a mechanical stimulus to the cells. 500 μL of 2×10^6 cells mL^{-1} of BMSCs was loaded onto the sterilized scaffold and allowed to infiltrate into it. After 5 mL of culture medium had been added, the cell-seeded scaffold was cultured at 37°C in a 5% CO_2 atmosphere for 1 day. The seeded scaffold was then placed in a spinner flask containing a differentiation medium with a magnetic stirring bar at 70 rpm for 10 h, and then at 50 rpm for 1, 2, and 4 weeks. The differentiation medium comprised high-glucose DMEM that was supplemented with 10% FBS, 1% penicillin/ streptomycin, 3.7 g L^{-1} sodium bicarbonate, 0.11 g L^{-1} sodium pyruvate,

50 μg mL^{-1} L-ascorbic acid (Sigma), 10mM β-glycerophosphate (Sigma), and 10^{-8} M dexamethasone (Sigma). The apparatus was placed in a CO_2 incubator. The medium was replaced every 3 days.

Biological response of rabbit calvarial bone

Experimental cranial implantation was conducted on 20 adult male New Zealand white rabbits. All animals were anaesthetized by intramuscular injections of a combination of ketamine and 2% Rompun solution. The head of each rabbit was shaved and sterilized with 10% povidone-iodine solution (Chou Jen Pharmaceutical Co., Nantou, Taiwan). The cranial surface was exposed by making a midline incision, and the overlying parietal periosteum was then excised. A full-thickness circular defect of the parietal bone with a diameter of 15 mm was created using a drilling burr. The calvarial bone defects were filled with the sterile GGT and GGT-GSB scaffolds to evaluate their osteogenerative characteristics.

Anesthetized animals were sacrificed post-operatively by administering an overdose of sodium pentobarbital at 8 weeks. Craniectomy sites where 2–3 mm of contiguous bone was present were removed from each skull. Cells were observed with an SEM. The sample was fixed in 10 wt % neutral-buffered formalin solution (Merck, Whitehouse Station, NJ) for 48 h, washed in phosphate-buffered saline (PBS), and dehydrated in a graded series of ethanol solutions. The sample was critically point-dried, coated with gold, and imaged using an SEM.

Bone defect repair was radiographically and histologically evaluated. Specimens were fixed using 10% phosphate-buffered formalin solution for 48 h. They were then radiographed using an X-ray apparatus (MGU 100A, TOSHIBA Co., Japan) with a high contrast X-ray film at 22 keV, 10 mA for 40 s. The radiographic appearance of a calcified mass revealed new bone. The regenerated bone was quantified using a semiautomatic histomorphometric method.[12] A satisfactory contrast was achieved between the implanted materials and the new bone tissue by setting gray level sensitivity standards that were consistent across all

treatments in an image analyzer system (Image-Pro Lite, Media Cybernetics, Silver Spring, MD). The image analyzer system, coupled to the microscope, was equipped with a phonic drawing tube, through which the image of the digitizing plate was projected over the optical field. The amount of new bone tissue was calculated by moving a cursor (was calculated at the location of the cursor) on the digitizing plate, which was made visible by projection over the histological field, and was expressed as a percentage of the in-grown bone tissue in the created bone defect. For histological analysis, all calvarial specimens were subsequently decalcified in a commercial medium (TBD-1 Rapid Decalcifier, Thermo Shandon, Pittsburgh, PA) for 24 h. They were dehydrated in a graded series of ethanol solutions and then embedded in paraffin (Merck, Whitehouse Station, NJ). Longitudinal sections of decalcified bone and implant (each 10 μm-thick) were prepared and stained with hematoxylin and eosin (H&E; Sigma). Sections were observed under an optical microscope (Axiovert 25; Carl Zeiss Inc., Göettingen, Germany).

Statistical Analysis

All quantitative data were presented as mean ± standard derivation. Statistical analysis was performed using a Student's *t*-test or one-way analysis of variance followed by *post hoc* Fisher's least significant difference test for multiple comparisons. A difference was deemed significant at $p < 0.05$. Before each statistical test, normal distribution was verified by normal probability plots.

RESULTS

Characteristics of the GGT and GGT-GSB scaffolds

Figure 1 presents SEM images of the cross-sectional scaffolds. Both GGT and GGT-GSB scaffolds exhibited similar three-dimensionally interconnected porous structure. The homogeneously distributed pores had pore sizes in the range 280-430 μm, which is close to

the size of the salt particles used. This result indicates that the salt particles determine the size of pores in the scaffold. Macropores in the scaffold were formed in the spaces that had been previously occupied by the salt particles. Additionally, numerous micropores were present in the macroporous walls, which were formed during freeze-drying.

The porosities of the GGT and GGT-GSB scaffolds were determined to be approximately 82.1% ± 1.5% and 80.5% ± 0.7%, respectively, revealing that the presence of GSB did not influence the porosity significantly ($p > 0.05$).

In vitro hydrolytic degradation of the crosss-linked GGT and GGT-GSB scaffolds continued for 8 weeks (Fig. 2). No notable difference was observed between GGT and GGT-GSB, suggesting that the addition of GSB did not influence degradation. Most of the non-cross-linked gelatin molecules and their adherent β-TCP particles were dissolved and released in the first week of soaking. The curves indicated that the degradation rates were attenuated after 1 week of soaking, even after the scaffolds had been soaked in deionized water for 8 weeks. The percentage weight remaining declined to 96% at week 8.

Biological response of rabbit calvarial bone

GGT-GSB and GGT scaffolds with and without BMSCs were implanted into bony defects in the calvariae of rabbits. All animals survived throughout the experiment. Gross observation of the whole calvaria 8 weeks post-implantation revealed that the GGT-GSB scaffold was intimately incorporated into the surrounding host bone (Fig. 3(A)). The skull bone-covered implant was removed from the transplantation site to determine whether the GGT-GSB scaffold had harmed underlying brain tissues. No sign of adverse reactions, such as cortical inflammation, necrosis or scar formation, was observed in the brain tissues beneath the GGT-GSB scaffold (Fig. 3(B)). The results demonstrate that the GGT-GSB scaffold did not cytotoxically affect the underlying brain tissues.

The formation of vessels in the GGT-GSB scaffold was visualized with an SEM (Fig. 4(A)).

Figure 4(B) shows numerous erythrocytes within the newly formed blood vessel at week 8. These results indicate that the porous GGT-GSB scaffold induced an angiogenic response in the host tissue, resulting in vascularization of the implant. After 8 weeks of implantation, the osteoblasts were observed to have attached around the periphery of the BMSCs-seeded GGT-GSB scaffold at 2 weeks of dynamic culture (Fig. 4(C)). Furthermore, many osteoblasts grew in the pores of the implant, revealing that the GGT-GSB scaffold had high cellular affinity and cyctocompatibility (Fig. 4(D)).

Figure 5 displays X-ray radiographs of 15 mm-wide skull defects in rabbits 8 weeks after the application of GGT and GGT-GSB scaffolds. New bone was present at the periphery of all GGT and GGT-GSB scaffolds with and without BMSCs. The new bone had partially replaced the scaffold, revealing that the volume of the scaffold had decreased. Additionally, the rounded bone defect became irregularly shaped. These results demonstrate the excellent tissue compatibility and osteoconduction of these scaffolds. However, a gap was present between the calvarial host bone and the acellular GGT scaffold (Fig. 5(A)). In contrast, defects that were repaired with acellular GGT-GSB (Fig. 5(E)) scaffold and BMSCs-seeded scaffolds (Fig. 5(B-D, F-H)) exhibited almost complete radiopacity at the interface between the calvaria host bone and the scaffold. These results indicate that the rate of biodegradation of all of the scaffolds, except for the acellular GGT scaffold, closely matched the rate of generation of new bone. Therefore, these implants were not visibly separate from the adjacent host calvarium at 8 weeks post-operation. Statistical analysis indicates that the area of the newly regenerated bone using the BMSCs-seeded scaffolds significantly exceeded that using acellular scaffolds (Fig. 6). Moreover, the GGT-GSB groups markedly accelerated bone regeneration over that achieved using GGT groups over the same period of dynamic culture, indicating that the release of GSB from the degraded scaffold promoted new bone growth. Furthermore, the area of new bone increased with the duration of the dynamic culture. However, the area of new

bone in defects that were treated with BMSCs-seeded scaffolds for 2 weeks of dynamic culture exhibited did not differ significantly from that after 4 weeks of dynamic culture. Based on this observation, the 2-week culture time point was adopted for the subsequent histological study.

Histological examination was performed 8 weeks post-operatively to characterize the osteogenic ability of the GGT-GSB scaffold and BMSCs-seeded GGT-GSB scaffold with 2 weeks of dynamic culture. Newly formed bone was observed at the periphery of the calvarila bone defects. A comparison with the cells-free GGT-GSB scaffold (Fig. 7(A)) revealed significantly more new bone formation at the periphery of the BMSCs-seeded GGT-GSB scaffold (Fig. 7(B)). The histological finding was consistent with the radiographic findings. Additionally, islands of bone growth were observed in the center of the defects that were repaired using the BMSCs-seeded GGT-GSB scaffold, replacing significant amounts of it (Fig. 7(C)). This result reveals that the seeded autologous BMSCs promoted the formation of new bone within the scaffold.

DISCUSSION

An effective bone scaffold should exhibit osteoconduction and osteoinduction. Gelatin has been identified as a substrate for cell adhesion and proliferation. β-TCP has been found to be osteoconductive. The authors' group previously developed a bone substitute composite of genipin-cross-linked gelatin and β-TCP. The substances gradually released from the composite facilitated the differentiation and proliferation of the osteoblasts.[11] Results of *in vivo* evaluation reveal that the composite had excellent biocompatibility and osteoconduction for the regenerating bone tissues.[12,22] However, the composite was not osteoinductive. Adding an osteoinductive agent or cells favorably accelerates the in-growth of new bone into a defect site. In addition, the composite had a lower porosity (68% ± 2.5%) after adding genipin. High porosity and large pores in a scaffold favor the sufficient supply of nutrients and oxygen, and

the in-growth and vascularization of cells and new bone tissue.

Salt leaching is a very simple approach for producing porous scaffolds with desired porous characteristics. Salts can exist as solid particles in aqueous media above the saturation concentration. Gross et al. founded that larger pores can be formed using larger salt particles.[23] Lee et al. used salt particles of size 300-500 μm to prepare gelatin scaffolds with an interconnected macroporous structure (average pore size = 350μm).[24] Accordingly, in this investigation, GGT scaffolds with macroporous structures were prepared by chemically cross-linking gelatin/β-TCP mixtures with genipin in the presence of salt particles of size 250-470 μm. The scaffold had a homogeneous pore structure and a high porosity (~80%). The pore sizes in GGT and GGT-GSB scaffolds were 280-430 μm. de Groot demonstrated that the optimal pore size for the in-growth of bone was approximately 200-500 μm.[25] Druecke et al. found that scaffolds with large pores of size 250-300 μm exhibited a significantly higher vessel density and faster vessel in-growth than those with smaller pores.[26] High porosity, large pores, and a three-dimensionally interconnected pore structure in the GGT-GSB scaffold provides a large surface area for the attachment of cells and adequate space for the in-growth of new bone tissue and the vascularization of the scaffold following implantation into the host tissue.

Several studies have demonstrated an improvement in clinical association with the use of GSB in the treatment of bone diseases. Furthermore, GSB promotes the proliferation and differentiation of bone cells as well as formation of nodules; it also accelerates tissue calcification.[14-16,18,20] Naringin, a polymethoxylated flavonoid, is reportedly the main effective component of GSB. It increases the amount of bone morphogenetic protein (BMP) in osteoblasts. Zhang et al. revealed that naringin can promote the proliferation and osteogenic differentiation of human BMSCs.[27] Jeong et al. found that GSB induced osteoblastic differentiation and considerably increased mineralization in osteoblastic cells.[18] The addition

of GSB significantly increased alkaline phosphatase (ALP) activity and stimulated the mineralization of an extracellular matrix in rat bone marrow cell culture. Wang et al. found that the extract and the active components of GSB promote the proliferation of UMR106 osteoblastic cells.[15] These findings suggest that GSB can enhance the proliferation and differentiation of cells.

Our previous study demonstrated that the osteoconductive activity of GGT composite could be responsible for the formation of bone around it.[12] To promote bone regeneration further, in this investigation, GSB was mixed with GGT and then seeded with autologous BMSCs. A spinner flask was utilized to culture the tissue engineering bone *in vitro*. Autologous BMSCs were used to prevent immune rejection of the transplanted cells. The *in vivo* bone growth-promoting capacity of the porous scaffold containing GSB and autologous BMSCs was evaluated in a rabbit calvarial defect model. Many researchers have confirmed that skull defects will not heal spontaneously when the defect is larger than 8 mm. Such defects are therefore good delayed-healing models.[28] As the scaffolds degraded, some of their constituents were released into the defects. The brain tissues beneath the GGT-GSB scaffold did not exhibit any cortical inflammation or scar formation, indicating that GSB and residual genipin released from the GGT-GSB scaffold did not harm the surrounding bone tissues.

SEM observation shows that new blood vessels formed and numerous erythrocytes were present in the BMSCs-seeded GGT-GSB scaffold at week 8, revealing that blood vessels from the neighboring host tissues had successfully invaded the scaffold. The long-term survival and functionality of various cells in the scaffold depend on the formation of new blood vessels.[29] The newly formed blood vessels can supply oxygen and nutrients that are required for the growth of cells. Insufficient vascularization will limit the formation of new bone and delay bone healing.[30] Hence, large tissue-engineered constructs must be vascularized before they can be applied clinically. The SEM image displays numerous osteoblasts around the pores in

the autologous BMSCs-seeded GGT-GSB scaffold 8 weeks post-implantation. The cells that differentiated into bone-forming osteoblasts were probably derived from the seeded autologous BMSCs. The release of gelatin, calcium, and GSB from the GGT-GSB scaffold facilitated their growth. These results demonstrate that the seeded autologous BMSCs, post-repair vascularization, and the release of nutritious elements from the scaffold may be responsible for the abundant proliferation of the cells at the cranial bone defect. These regenerating cells may modulate further development of bone tissue.

The result of *in vitro* degradation of scaffolds in deionized water demonstrated that the weight loss of the scaffold was only 4% for 8 weeks. The weight loss was primarily due to the dissolution and hydrolysis of the scaffold. However, gelatin is readily degraded by proteolytic enzymes (proteases) in the body.[31] Moreover, β-TCP could be degraded by cell phagocytosis.[32] In this study, radiographic and histological analyses verified the growth of new bone into the calvarium defects in the porous GGT and GGT-GSB scaffolds after 8 weeks of implantation. Moreover, defects treated with acellular GGT-GSB scaffold and BMSCs-seeded scaffolds exhibited almost complete radiopacity at the interface between the calvaria host bone and the scaffold. These results indicate that the rate of biodegradation of these scaffolds closely matched the rate of generation of new bone.

Quantitative histomorphometric analysis revealed that a porous GGT scaffold with autologous BMSCs promoted the formation of new bone tissue at the defect site beyond that achieved using an acellular scaffold. At 8 weeks after surgery, new bone had filled 17.1% of the acellular GGT defects and 23.0%-30.2% of defects with the BMSCs-seeded GGT scaffolds with different periods of dynamic culture (1, 2, and 4 weeks). SEM examination revealed regenerating osteoblasts in the peripheral and central areas of the BMSCs-seeded scaffold. Additionally, examination of the H&E-stained sections of the craniectomy sites revealed that new bone replaced a significant amount of GGT-GSB scaffold, suggesting that

the autologous BMSCs were responsible for bone formation at their locations. Previous investigations have established that the combination of autologous BMSCs with a scaffold can accelerate bone healing. For example, Wang et al. adopted autologous BMSCs in conjunction with β-TCP scaffolds to repair segmental bone defects in goat tibias.[2] At 24 weeks post-operation, the percentage of new bone volume for the scaffold cultured by dynamic perfusion bioreactor (76%-83%) was higher than that cultured in static state (40%-49%). Yoshii et al. identified new bone formation in most fresh autologous bone marrow-seeded porous β-TCP; however, they detected no bone formation in β-TCP unless bone marrow was introduced.[3] At 5 and 10 weeks after implantation in rabbit intramuscular sites, the percentage of bone formation area for granule β-TCP scaffolds with bone marrow was about 8%. Mankani et al. reconstructed canine cranial using autologous BMSCs-containing hydroxyapatite/TCP and found that a BMSCs-containing transplant formed significantly more bone than a BMSCs-free transplant.[4] Similarly, den Boer et al. added autologous BMSCs to porous hydroxyapatite to heal segmental bone defects.[5] They showed that the addition of fresh autologous bone marrow considerably improved healing. The cited studies indicated that the use of autologous BMSCs with scaffolds can increase the bone healing capacity of those scaffolds, probably because the BMSCs reduce the time required for the cells to invade defect sites.

In this investigation, the area of regenerated bone as a percentage of total area of calvarial bone defect achieved using GGT-GSB scaffolds exceeded that achieved using GGT groups for the same period of dynamic culture. At 8 weeks following implantation, the percentage of the newly formed bone for the GGT scaffold was 28.5% ± 2.0% and that for the GGT-GSB scaffold was 34.2% ± 2.4% when the period of dynamic culture was 2 weeks. GSB was gradually released from the biodegradable scaffold, and was thought positively to affect bone regeneration. This observation is consistent with findings of previous studies. For instance,

Wong and Rabie showed that more new bone was formed in the parietal bone defect of rabbit when GSB extract was used in collagen graft than when autogenous endochondral bone alone or collagen alone was used in graft.[33] Jeong et al. suggested that GSB promotes the formation of new bone by regulating BMP-2, ALP, and type I collagen.[18] Hung et al. founded that GSB promotes osteoblast mineralization by inducing bone differentiation-related gene expression.[34] As described in the present authors' earlier work, adding GSB made GGT composite simultaneously osteoconductive and osteoinductive.[19] These results reflect the fact that GSB can induce the formation of new bone by providing an effective biodegradable delivery system.

In summary, porous biodegradable GGT-GSB scaffolds with pore size of 280-430 μm were successfully prepared using a salt-leaching method. An autologous BMSCs-seeded GGT-GSB scaffold was used to fill a critically sized bone defect in a rabbit calcarial model. It successfully promoted bone regeneration with good osteoconductive potential. Accordingly, incorporating GSB and autologous BMSCs to a porous GGT scaffold makes it ideal for bone formation.

ACKNOWLEDGMENTS

The authors would like to thank the National Science Council of the Republic of China, Taiwan (contract No. NSC 98-2221-E-039-005-MY3) and the China Medical University (contract No. CMU99-S-44) for financially supporting this research.

REFERENCES

1. Bruder SP, Jaiswal N, Ricalton NS, Mosca JD, Kraus KH, Kadiyala S. Mesenchymal stem cells in osteobiology and applied bone regeneration. Clin Orthop Rel Res 1998;355:S247–S256.
2. Wang C, Wang Z, Li A, Bai F, Lu J, Xu S, Li D. Repair of segmental bone-defect of goat's tibia using a dynamic perfusion culture tissue engineering bone. J Biomed Mater Res A 2010;92:1145–1153.
3. Yoshii T, Sotome S, Torigoe I, Tsuchiya A, Maehara H, Ichinose S, Shinomiya K. Fresh bone marrow introduction into porous scaffolds using a simple low-pressure loading method for effective osteogenesis in a rabbit model. J Orthop Res 2009;27:1–7.

4. Mankani MH, Kuznetsov SA, Shannon B, Nalla RK, Ritchie RO, Qin Y, Robey PG. Canine cranial reconstruction using autologous bone marrow stromal cells. Am J Pathol 2006;168:542–550.
5. den Boer FC, Wippermann BW, Blokhuis TJ, Patka P, Bakker FC, Haarman HJ. Healing of segmental bone defects with granular porous hydroxyapatite augmented with recombinant human osteogenic protein-1 or autologous bone marrow. J Orthop Res 2003;21:521–528.
6. Rim NG, Lee JH, Jeong SI, Lee BK, Kim CH, Shin H. Modulation of osteogenic differentiation of human mesenchymal stem cells by poly[(L-lactide)-co-(ε-caprolactone)]/gelatin nanofibers. Macromol Biosci 2009;9:795–804.
7. Bernhardt A, Despang F, Lode A, Demmler A, Hanke T, Gelinsky M. Proliferation and osteogenic differentiation of human bone marrow stromal cells on alginate-gelatine-hydroxyapatite scaffolds with anisotropic pore structure. J Tissue Eng Regen Med 2009;3:54–62.
8. Zhao F, Grayson WL, Ma T, Bunnell B, Lu WW. Effects of hydroxyapatite in 3-D chitosan-gelatin polymer network on human mesenchymal stem cell construct development. Biomaterials 2006;27:1859–1867.
9. Takahashi Y, Yamamoto M, Tabata Y. Osteogenic differentiation of mesenchymal stem cells in biodegradable sponges composed of gelatin and β-tricalcium phosphate. Biomaterials 2005;26:3587–3596.
10. Takahashi Y, Yamamoto M, Tabata Y. Enhanced osteoinduction by controlled release of bone morphogenetic protein-2 from biodegradable sponge composed of gelatin and β-tricalcium phosphate. Biomaterials 2005;26:4856–4865.
11. Liu BS, Yao CH, Chen YS, Hsu SH. *In vitro* evaluation of degradation and cytoxicity of a novel composite as a bone substitute. J Biomed Mater Res A 2003;67:1163–1169.
12. Yao CH, Liu BS, Hsu SH, Chen YS. Calvarial bone response to a tricalcium phosphate-genipin crosslinked gelatin composite. Biomaterials 2005;26:3065–3074.
13. Wong RWK, Rabie ABM. Traditional Chinese medicines and bone formation–A review. J Oral Maxillofac Surg 2006;64:828–837.
14. Dong GC, Chen HM, Yao CH. A novel bone substitute composite composed of tricalcium phosphate, gelatin and *Drynaria fortunei* herbal extract. J Biomed Mater Res A 2008;84:167–177.
15. Wang XL, Wang NL, Zhang Y, Gao H, Pang WY, Wong MS, Zhang G, Qin L, Yao XS. Effects of eleven flavonoids from the osteoprotective fraction of *Drynaria fortunei* (Kunze) J. Sm. on osteoblastic proliferation using an osteoblast-like cell line. Chem Pharm Bull 2008;56:46–51.
16. Jeong JC, Lee JW, Yoon CH, Lee YC, Chung KH, Kim MG, Kim CH. Stimulative effects of *Drynariae Rhizoma* extracts on the proliferation and differentiation of osteoblastic MC3T 3-E1 cells. J Ethnopharmacol 2005;96:489–495.
17. Yin J, Tezuka Y, Kouda K, Tran Q, Miyahara T, Chen Y, Kadota S. Antiosteoporotic activity of the water extract of *Dioscorea spongiosa*. Biol Pharm Bull 2004;27:583–586.
18. Jeong JC, Lee JW, Yoon CH, Kim HM, Kim CH. *Drynariae Rhizoma* promotes osteoblast differentiation and mineralization in MC3T3-E1 cells through regulation of bone

morphogenetic protein-2, alkaline phosphatase, type I collagen and collagenase-1. Toxicol in Vitro 2004;18:829–834.

19. Jeong JC, Kang SK, Youn CH, Jeong CW, Kim HM, Lee YC, Chang YC, Kim CH. Inhibition of *Drynariae Rhizoma* extracts on bone resorption mediated by processing of cathepsin K in cultured mouse osteoclasts. Int Immunopharmacol 2003;3:1685–1697.
20. Sun JS, Lin CY, Dong GC, Sheu SY, Lin FH, Chen LT, Wang YJ. The effect of Gu-Sui-Bu (*Drynaria fortunei* J. Sm) on bone cell activities. Biomaterials 2002;23:3377–3385.
21. Lin CY, Sun JS, Sheu SY, Lin FH, Wang YJ, Chen LT. The effect of Chinese medicine on bone cell activities. Am J Chin Med 2002;30:271–285.
22. Yao CH, Liu BS, Hsu SH, Chen YS, Tsai CC. Biocompatibility and biodegradation of a bone composite containing tricalcium phosphate and genipin crosslinked gelatin. J Biomed Mater Res A 2004;69:709–717.
23. Gross KA, Rodríguez-Lorenzo LM. Biodegradable composite scaffolds with an interconnected spherical network for bone tissue engineering. Biomaterials 2004;25:4955–4962.
24. Lee SB, Kim YH, Chong MS, Hong SH, Lee YM. Study of gelatin-containing artificial skin V: Fabrication of gelatin scaffolds using a salt-leaching method. Biomaterials 2005;26:1961–1968.
25. de Groot K. Bioceramics consisting of calcium phosphate salts. Biomaterials 1980;1:47–50.
26. Druecke D, Langer S, Lamme E, Pieper J, Ugarkovic M, Steinau HU, Homann HH. Neovascularization of poly(ether ester) block-copolymer scaffolds *in vivo*: Long-term investigations using intravital fluorescent microscopy. J Biomed Mater Res A 2004;68:10–18.
27. Zhang P, Dai KR, Yan SG, Yan WQ, Zhang C, Chen DQ, Xu B, Xu ZW. Effects of naringin on the proliferation and osteogenic differentiation of human bone mesenchymal stem cell. Eur J Pharmacol 2009;607:1–5.
28. Schmitz JP, Hollinger JO. The critical size defect as an experimental model for craniomandibulofacial nonunions. Clin Orthop Relat Res 1986;205:299–308.
29. Collin-Osdoby P. Role of vascular endothelial cells in bone biology J Cell Biochem 1994;55:304–309.
30. Santos MI, Reis RL. Vascularization in bone tissue engineering: Physiology, current strategies, major hurdles and future challenges. Macromol Biosci 2010;10:12–27.
31. Yamamoto M, Ikada Y, Tabata Y. Controlled release of growth factors based on biodegradation of gelatin hydrogel. J Biomater Sci Polym Edn 2001;12:77–88.
32. Frayssinet P, Gineste L, Conte P, Fages J, Rouquet N. Short-term implantation effects of a DCPD-based calcium phosphate cement. Biomaterials 1998;19:971–977.
33. Wong RWK, Rabie ABM. Effect of Gusuibu graft on bone formation. J Oral Maxillofac Surg 2006;64:770–777.
34. Hung TY, Chen TL, Liao MH, Ho WP, Liu DZ, Chung WC, Chen RM. *Drynaria fortunei* J. Sm. promotes osteoblast maturation by inducing differentiation-related gene expression and protecting against oxidative stress-induced apoptotic insults. J Ethnopharmacol 2010;131:70–77.

FIGURE LEGENDS

Figure 1. SEM images of the cross-section morphologies of (A) GGT and (B) GGT-GSB scaffolds.

Figure 2. Weight loss of scaffolds during the soaking time.

Figure 3. (A) The GGT-GSB scaffold was contained in the implant site at 8 weeks post-surgery, and no evidence exists of clinical complications around the calvarial bone defect. (B) The brain tissues underlying the implantation site were found to display no evidence of adverse tissue reaction to the GGT-GSB scaffold.

Figure 4. SEM observation of BMSCs-seeded GGT-GSB scaffold after 8 weeks of post-implantation. (A) New blood vessel and (B) erythrocytes (EC) in the scaffold. Osteoblasts (OB) regenerating around (C) the peripheral part and (D) the central part of the scaffold (HB = host bone).

Figure 5. Radiographs of calvarial bone-covered implant removed after (A) porous GGT scaffold alone and cells-seeded GGT scaffolds with (B) 1, (C) 2, and (D) 4 weeks of dynamic culture were implanted into the calvarial bone defect for 8 weeks. Radiographs of calvarial bone-covered (E) porous GGT-GSB scaffold alone and cells-seeded GGT-GSB scaffolds with (F) 1, (G) 2, and (H) 4 weeks of dynamic culture (HB = host bone, NB = new bone). The dotted circles indicate the original defect.

Figure 6. The percentage of the area of the newly formed bone to the total area of the calvarial bone defect. (n = 3)

Figure 7. Histological images of H&E-stained (A) GGT-GSB scaffold and (B,C) cells-seeded GGT-GSB scaffolds with 2 weeks of dynamic culture implanted in calvarial defects for 8 weeks (HB = host bone, NB = new bone). Images (A) and (B) are peripheral part of implants. Image (C) is central part of implant.

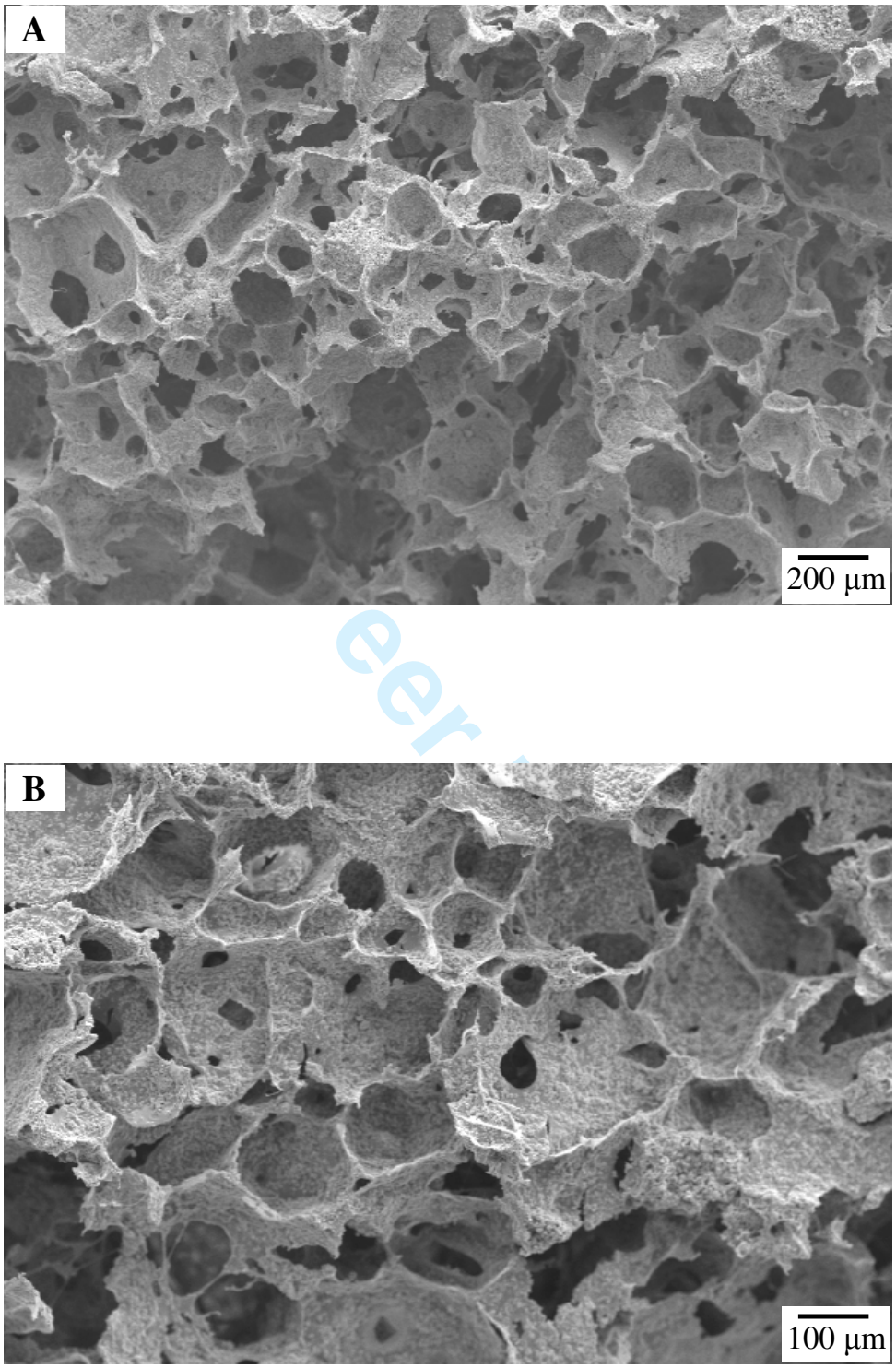

Figure 1.

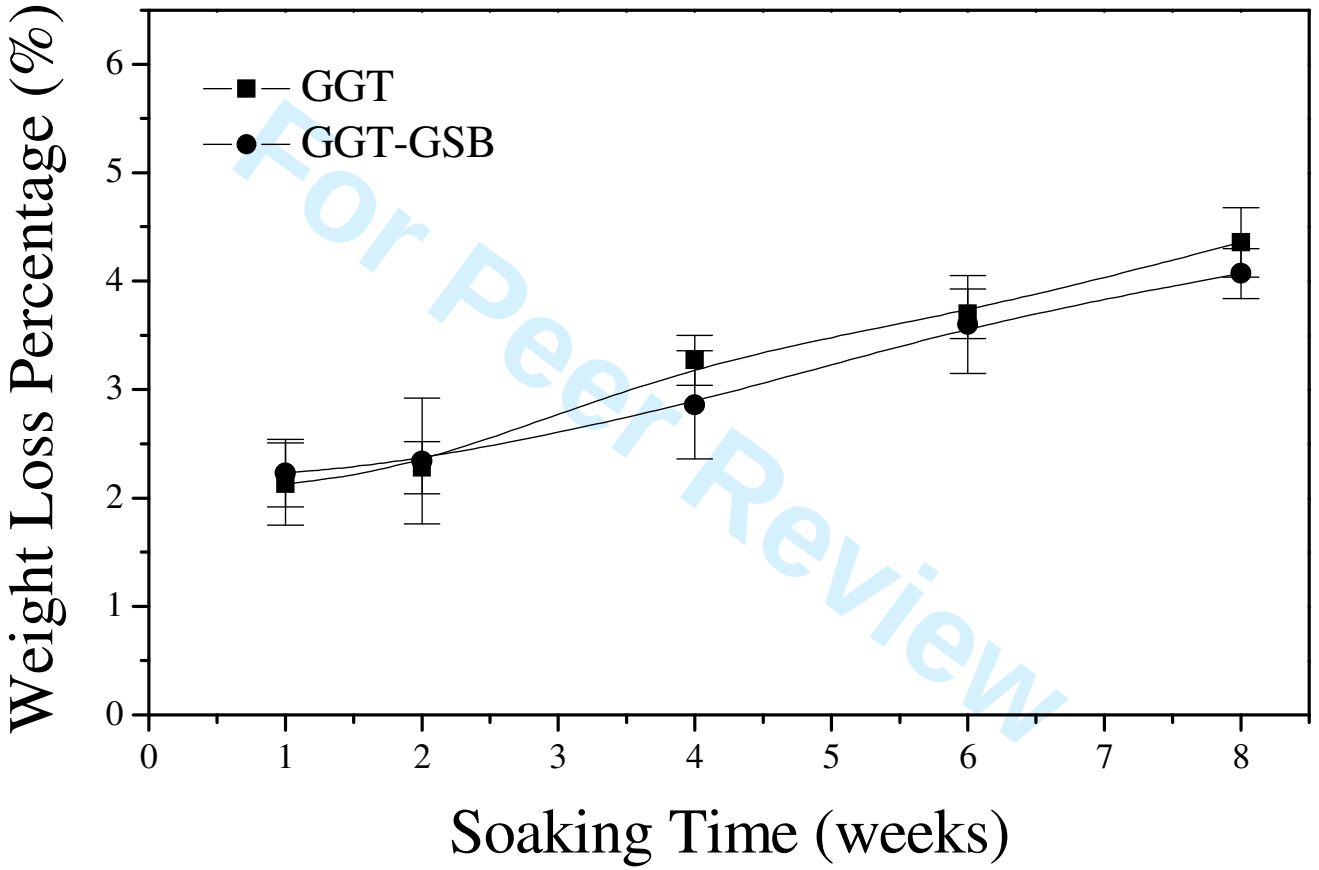

Figure 2.

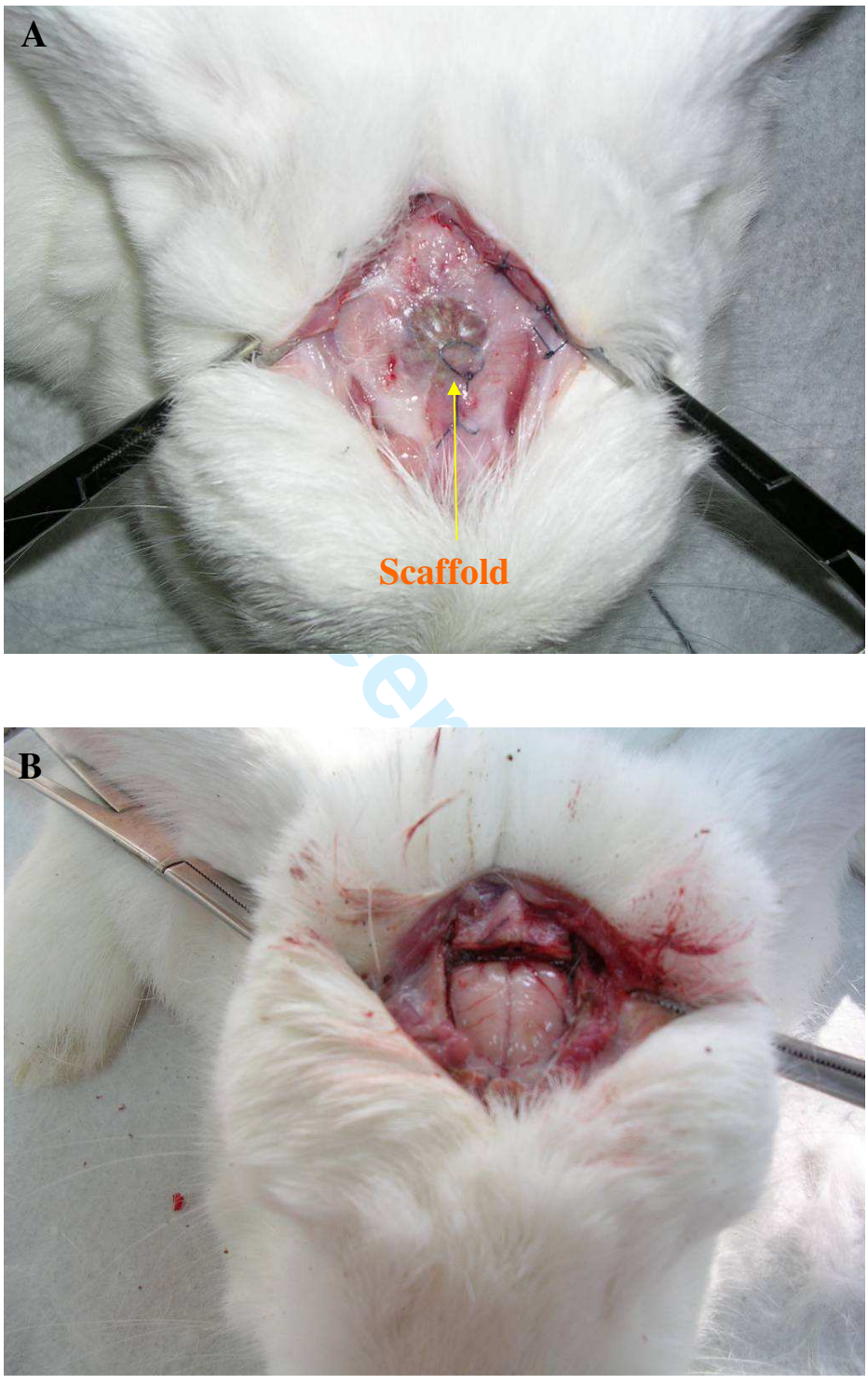

Figure 3.

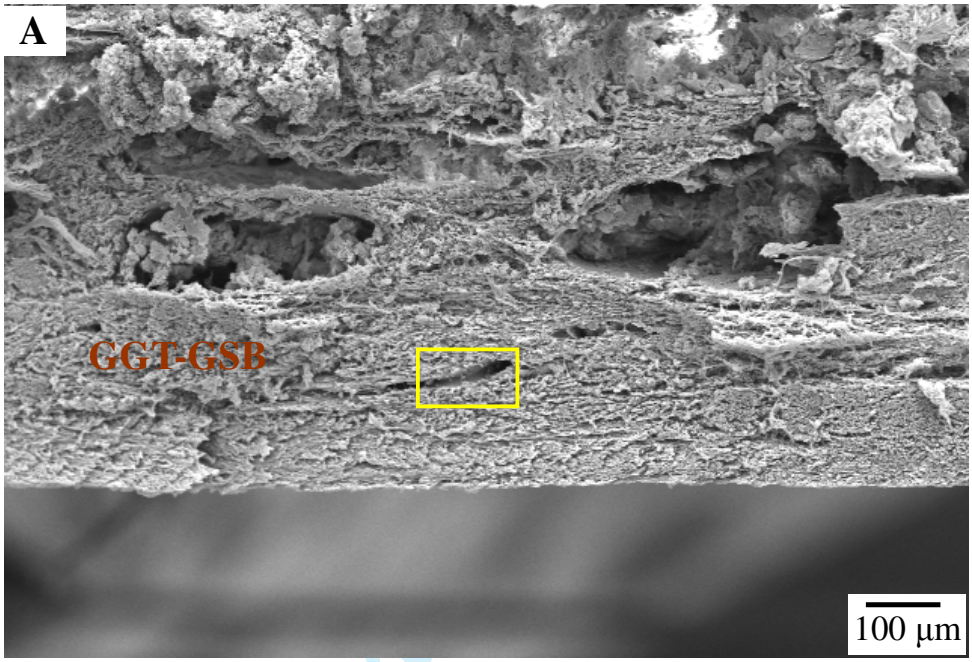
A
GGT-GSB
100 μm

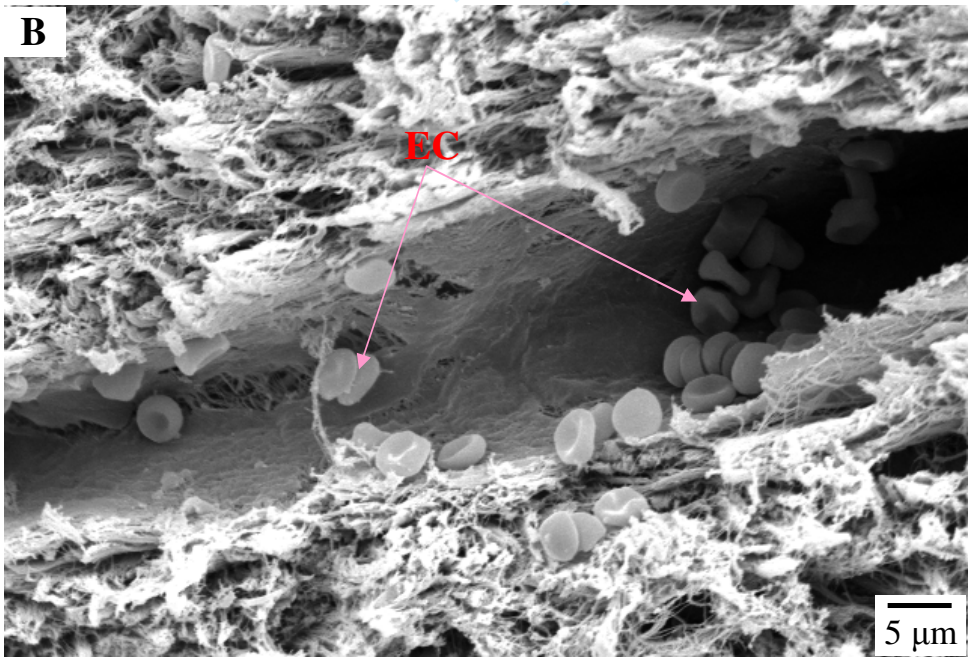
B
EC
5 μm

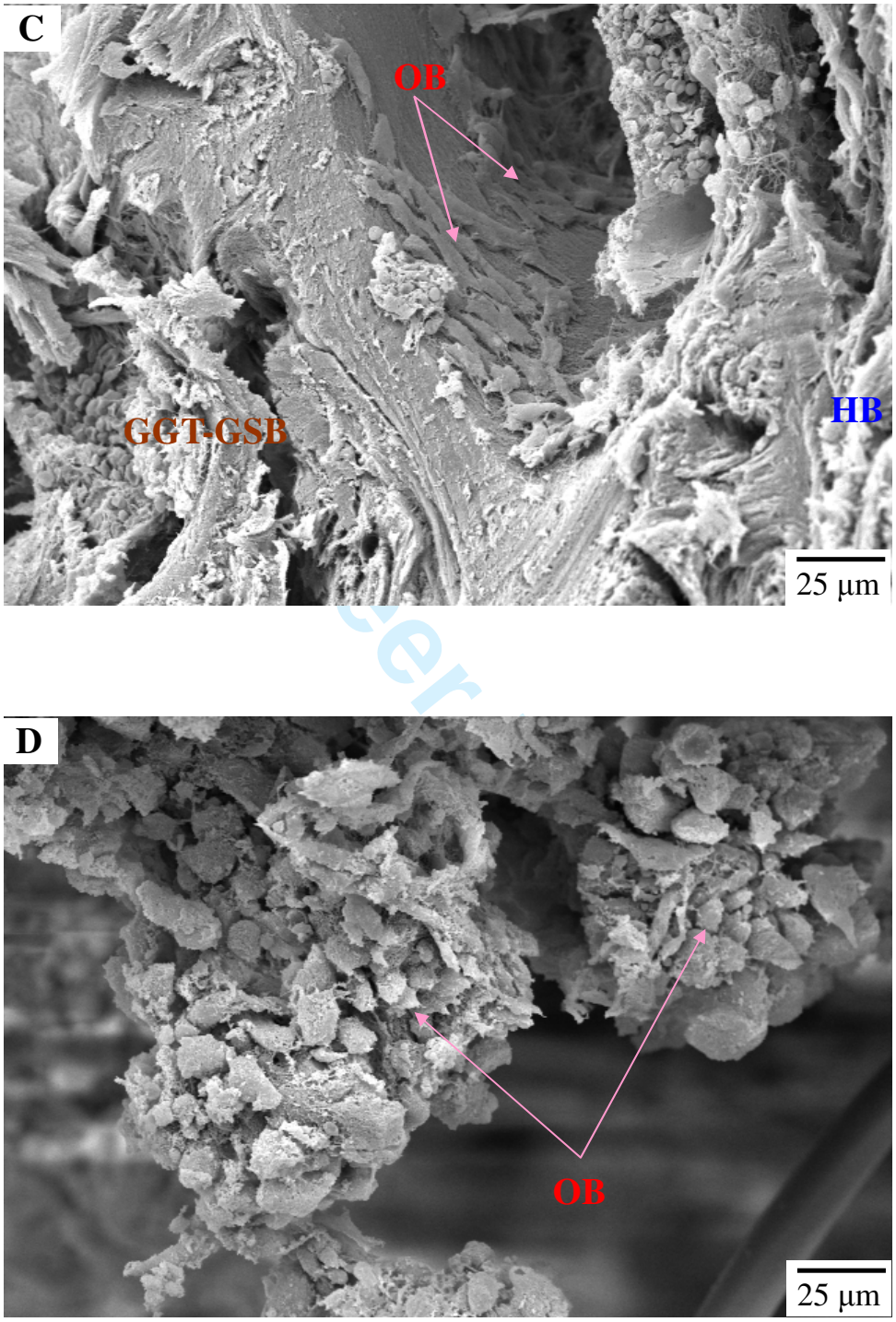

Figure 4.

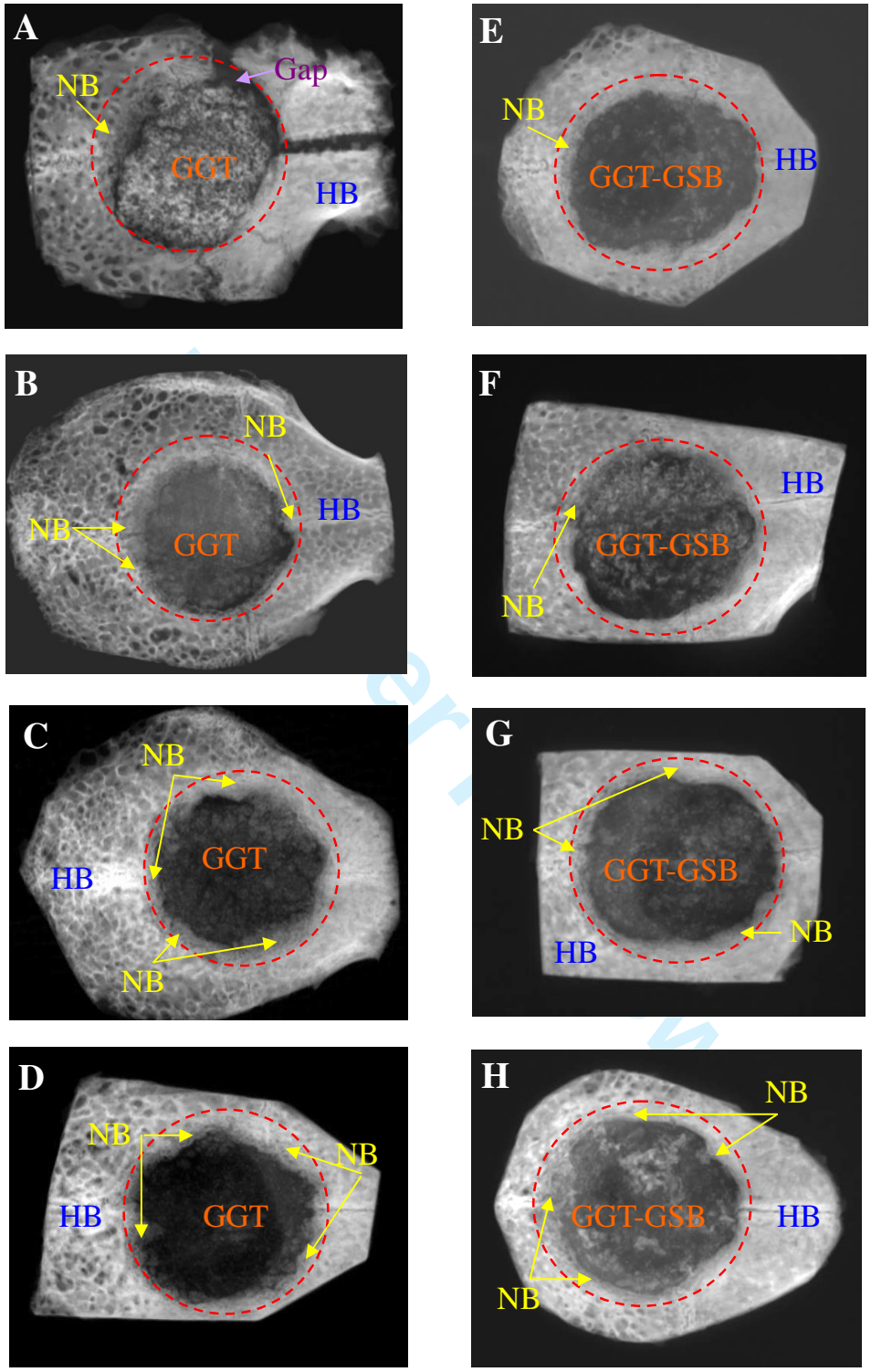
A
NB
Gap
GGT
HB
E
NB
GGT-GSB
HB
B
NB
HB
NB
GGT
F
HB
GGT-GSB
NB
C
NB
GGT
HB
NB
G
NB
GGT-GSB
NB
HB
D
NB
NB
HB
GGT
H
NB
GGT-GSB
HB
NB

Figure 5.

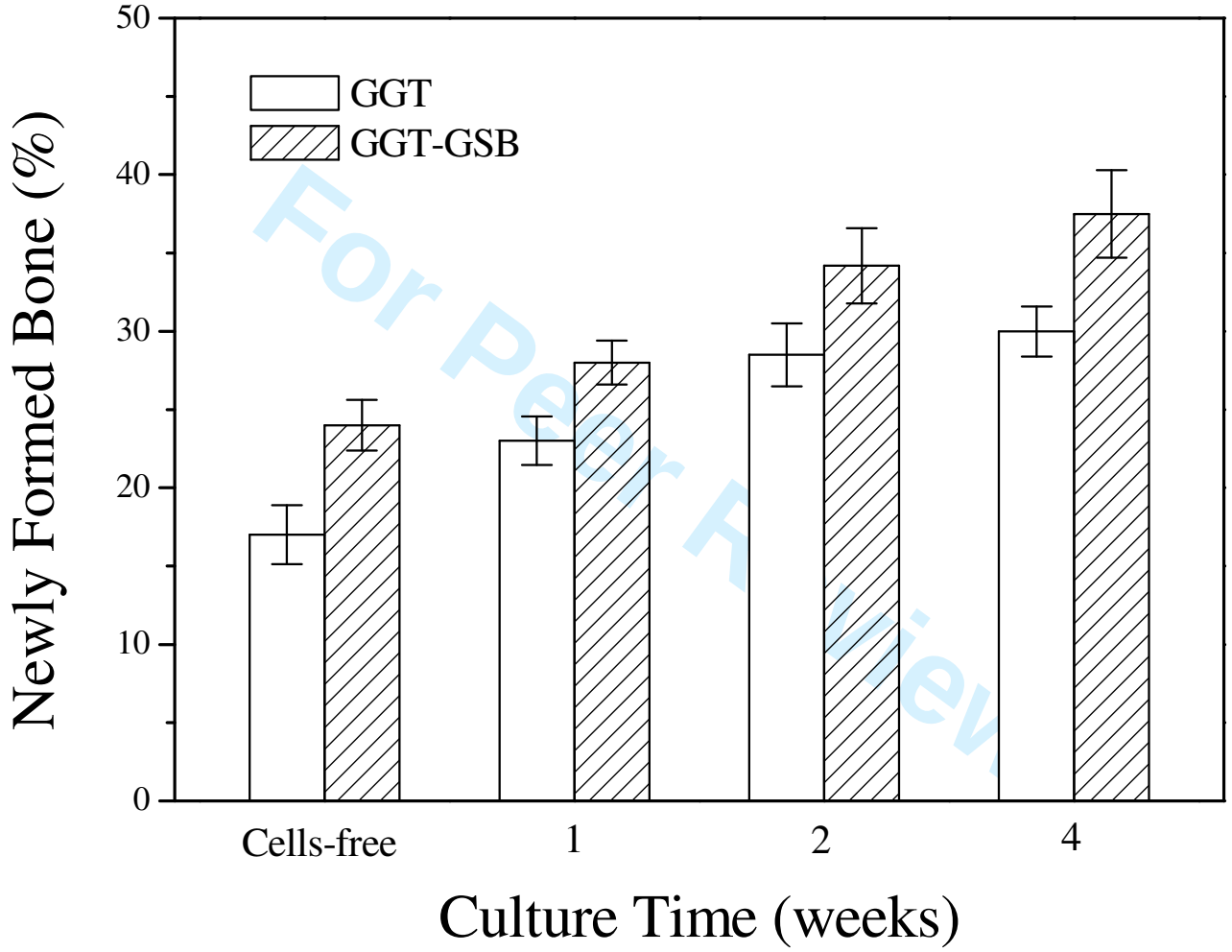

Figure 6.

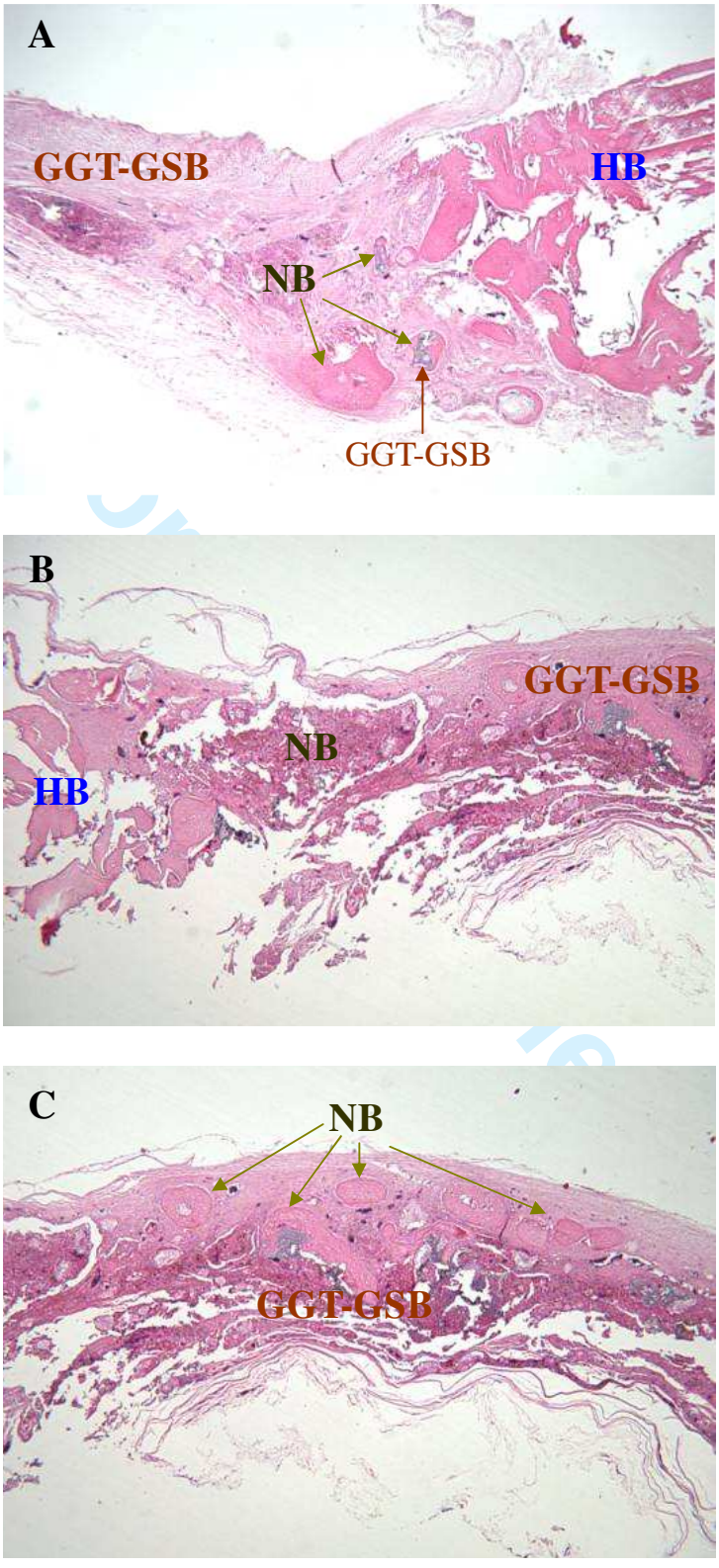

Figure 7.